Buoyancy-Affected Flows In Ventilated Rooms

Nielsen, Peter V.

Published in:
Numerical Heat Transfer, Part A

Publication date:
1979

Document Version
Early version, also known as pre-print

Numerical Heat Transfer, vol. 2, pp. 115-127, 1979

BUOYANCY-AFFECTED FLOWS IN VENTILATED ROOMS

P. V. Nielsen, A. Restivo, and J. H. Whitelaw
Department of Mechanical Engineering, Fluids Section,
Imperial College of Science and Technology, London SW7 2BX

Calculations of velocity and temperature distributions in rooms with ventilation arrangements are reported. The method involves the solution, in finite-difference form, of two-dimensional equations for the conservation of mass, momentum, energy, turbulence energy, and dissipation rate, with algebraic expressions for the turbulent viscosity and heat diffusivity. The results are shown to be in reasonable agreement with available experimental data and the method is then applied to provide additional information useful for design purposes.

INTRODUCTION

The main purpose of air-conditioning systems is to maintain a suitable distribution of air velocity, temperature, and humidity in some closed space, typically a room. The designer of ventilated rooms is required, therefore, to know in advance the flow characteristics of a given air-conditioning arrangement in a particular room geometry.

In the past, calculation methods have made use of extensive assumptions to estimate the velocity levels without actually solving the flow equations. At present, however, direct solution of the equations of motion, in time-averaged form and with modeled turbulent stresses, lies within reasonable limits of computer usage and cost, and the interest in this approach has increased rapidly. In a previous paper [1] the velocity characteristics of room and ventilation arrangements were calculated; the present contribution extends the method to allow the calculation of two-dimensional temperature distributions in ventilated rooms with buoyancy effects.

Temperature gradients are usually present as a result of heat transfer through walls and windows, heat generation by the room occupiers or heaters, or air at a different temperature being blown through the ventilation system. Energy is transported throughout the room as a passive property and interacts with the velocity field, inducing nonuniform buoyancy forces that affect both the mean flow and the turbulence. The effect of buoyancy is commonly expressed in air-conditioning literature by a global Archimedes number

The authors wish to acknowledge personal financial support from the Danish Government Fund for Scientific and Industrial Research (PVN) and from the Comissão Permanente INVOTAN and Instituto Nacional de Investigação Cientifica (AR). Danfoss A/S (PVN) and the University of Oporto (AR) kindly released their staff to allow this work to be carried out. The experimental and computational work was supported by the Science Research Council, to whom all the authors extend their thanks.

0149-5720/79/010115-13$2.75

NOMENCLATURE

a, b	boundaries surrounding inlet opening	x, y	coordinates
		x_R	abscissa of reattachment point
Ar	Archimedes number ($= \beta g h\, \Delta T_0 / U_0^2$)	β	coefficient of thermal expansion
		$\gamma_{h,t}$	turbulent heat diffusivity
B	buoyancy parameter $[= -\beta g (K/\epsilon)^2\, \partial\theta/\partial y]$	$\Gamma_{h,\text{eff}}$	effective exchange coefficient for heat
C_1, C_2, C_μ	constants in turbulence model	Γ_ϕ	exchange coefficient in ϕ equation
f	wall parameter in expression for σ_t	ΔT_0	temperature difference between outlet and inlet
g	gravitational acceleration		
G, G_B	generation of K by shear and buoyancy	ϵ	dissipation of turbulence kinetic energy
h	height of inlet slot	θ	excess temperature ($= T - T_0$)
H, L	dimensions of room or model	κ	von Kármán constant
K	turbulence kinetic energy	μ_{eff}, μ_t	effective and turbulent viscosities
P	pressure	ν	fluid laminar viscosity
Re	Reynolds number ($= h U_0 / \nu$)	ν_t	turbulent momentum diffusivity
S_ϕ	source term in ϕ equation	ρ	fluid density
T_0	inlet fluid temperature	σ	fluid Prandtl number
U, V	components of mean velocity	σ_t	turbulent Prandtl number
U_m	peak velocity across jet	$\sigma_k, \sigma_\epsilon$	constants in turbulence model
U_{rm}	maximum velocity in reverse flow	ϕ	general dependent variable
U_0	bulk inlet fluid velocity		

$$\text{Ar} = \frac{\beta g h\, \Delta T_0}{U_0^2}$$

with ΔT_0 the temperature difference between outlet and inlet, and h and U_0 a characteristic length and velocity of the diffuser employed.

Previous numerical studies of buoyancy-affected flows of this type include the works of Nielsen [2] and Larson [3] with a stream function-vorticity formulation. Experimental investigations have been reported, for example, by Linke [4], Jackman [5], Schwenke [6], Hestad [7], Nagasawa [8], and Nielsen [2], who provided qualitative information by flow visualization and quantitative information by the measurement of local values of temperature and velocity. In spite of numerous data, experiments with simple and known boundary conditions—for example, with one wall uniformly heated and the others adiabatic—are in short supply. Nevertheless, sufficient data exist to allow an appraisal of the present method.

The following section introduces the equations solved and the calculation method. Calculated results are presented and discussed and conclusions are drawn in the remaining sections.

EQUATIONS, BOUNDARY CONDITIONS, AND NUMERICAL PROCEDURE

The equations solved are the continuity, momentum (two components), and energy equations, written in time-averaged form and expressing the turbulent stresses and heat fluxes in terms of turbulent diffusivities for momentum ν_t and heat $\gamma_{h,t}$,

respectively. The two diffusivities are connected by the turbulent Prandtl number $\sigma_t = \nu_t/\gamma_{h,t}$ and the former is calculated in terms of the turbulent kinetic energy K and its dissipation rate ϵ,

$$\nu_t = \frac{C_\mu K^2}{\epsilon}$$

K and ϵ are derived from two additional transport equations. All differential equations are reducible to the general form

$$\frac{\partial}{\partial x}(\rho U\phi) + \frac{\partial}{\partial y}(\rho V\phi) = \frac{\partial}{\partial x}\left(\Gamma_\phi \frac{\partial \phi}{\partial x}\right) + \frac{\partial}{\partial y}\left(\Gamma_\phi \frac{\partial \phi}{\partial y}\right) + S_\phi$$

where ϕ, Γ_ϕ, and S_ϕ assume the values listed in Table 1, with

$$G = \mu_t \left\{ 2\left[\left(\frac{\partial U}{\partial x}\right)^2 + \left(\frac{\partial V}{\partial y}\right)^2\right] + \left(\frac{\partial U}{\partial y} + \frac{\partial V}{\partial x}\right)^2 \right\}$$

$$G_B = \rho\beta g \frac{\nu_t}{\sigma_t}\frac{\partial \theta}{\partial y}$$

θ is the excess temperature $T - T_0$, where T_0 is some reference value; the effective viscosity μ_{eff} is defined by

$$\mu_{\text{eff}} = \rho(\nu + \nu_t)$$

and the effective exchange coefficient for heat $\Gamma_{h,\text{eff}}$ by

$$\Gamma_{h,\text{eff}} = \rho\left(\frac{\nu}{\sigma} + \frac{\nu_t}{\sigma_t}\right)$$

Table 1 Values of ϕ, Γ_ϕ, S_ϕ and Buoyancy Terms

ϕ	Γ_ϕ	S_ϕ	Buoyancy
1	0	0 (continuity)	
U	μ_{eff}	$-\frac{\partial P}{\partial x} + \frac{\partial}{\partial x}\left(\mu_{\text{eff}}\frac{\partial U}{\partial x}\right) + \frac{\partial}{\partial y}\left(\mu_{\text{eff}}\frac{\partial V}{\partial x}\right)$	
V	μ_{eff}	$-\frac{\partial P}{\partial y} + \frac{\partial}{\partial x}\left(\mu_{\text{eff}}\frac{\partial U}{\partial y}\right) + \frac{\partial}{\partial y}\left(\mu_{\text{eff}}\frac{\partial V}{\partial y}\right)$	$-\rho\beta g\theta$
h	$\Gamma_{h,\text{eff}}$	0	
K	$\frac{\mu_{\text{eff}}}{\sigma_K}$	$G - \rho\epsilon$	$+ G_B$
ϵ	$\frac{\mu_{\text{eff}}}{\sigma_\epsilon}$	$\frac{\epsilon}{K}(C_1 G - C_2 \rho\epsilon)$	$+ C_1 \frac{\epsilon}{K} G_B$

Since temperature differences are small in air-conditioning applications (typically less than 10°C), the coefficient of volumetric expansion β was assumed constant, and the influence of density variations was neglected in terms that do not contribute to buoyancy effects. Buoyancy terms are listed in the last column of Table 1, for the vertical momentum equation (y axis directed vertically downward) and the K and ϵ equations. The terms in the momentum equations are exact and those in the K and ϵ equations have been modeled in the way proposed by Launder [9]. The turbulent heat fluxes have been expressed in terms of a turbulent diffusivity for heat, as in the energy equation. The turbulent Prandtl number σ_t has been made dependent on buoyancy, making use of an expression proposed by Gibson and Launder [10] for horizontal flows:

$$\sigma_t = 0.67 \frac{1 + 0.83f + 0.112f^2 + (0.267 + 0.242f)B}{1 + 0.417f + 0.093B}$$

where $f = (K^{3/2}/\epsilon)/c_\mu^{-3/4}\kappa d$, with d equal to the distance to the nearest boundary, accounts for the vicinity of walls and B is a parameter characteristic of the buoyancy effects, defined by

$$B = -\beta g \frac{K^2}{\epsilon^2} \frac{\partial \theta}{\partial y}$$

The five "constants" C_1, C_2, C_μ, σ_k, and σ_ϵ were assigned the values used in the earlier isothermal calculations, listed in [1].

The boundary conditions for the velocity and turbulence properties were similar to those in [1]; i.e., zero gradients in the exit plane and in plane b of Fig. 1, prescribed values in plane a of Fig. 1, and turbulent wall functions to describe the near-wall regions close to all solid surfaces. In addition, identical conditions were imposed on the temperature in the exit plane and planes a and b, and all surfaces were assumed adiabatic except the bottom one, where a uniform heat flux distribution was prescribed. The wall functions, similar to those in [1], need not be extended to the temperature for this type of boundary condition.

The equations were solved in finite-difference form with the computer program TEACH, first described by Gosman and Pun [11] and extensively used by several workers at Imperial College. Calculations were performed in a CDC 6600 computer,

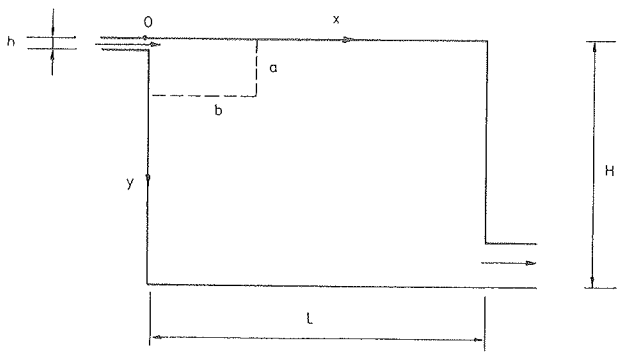

Fig. 1 Boundaries of calculated flows and coordinate system.

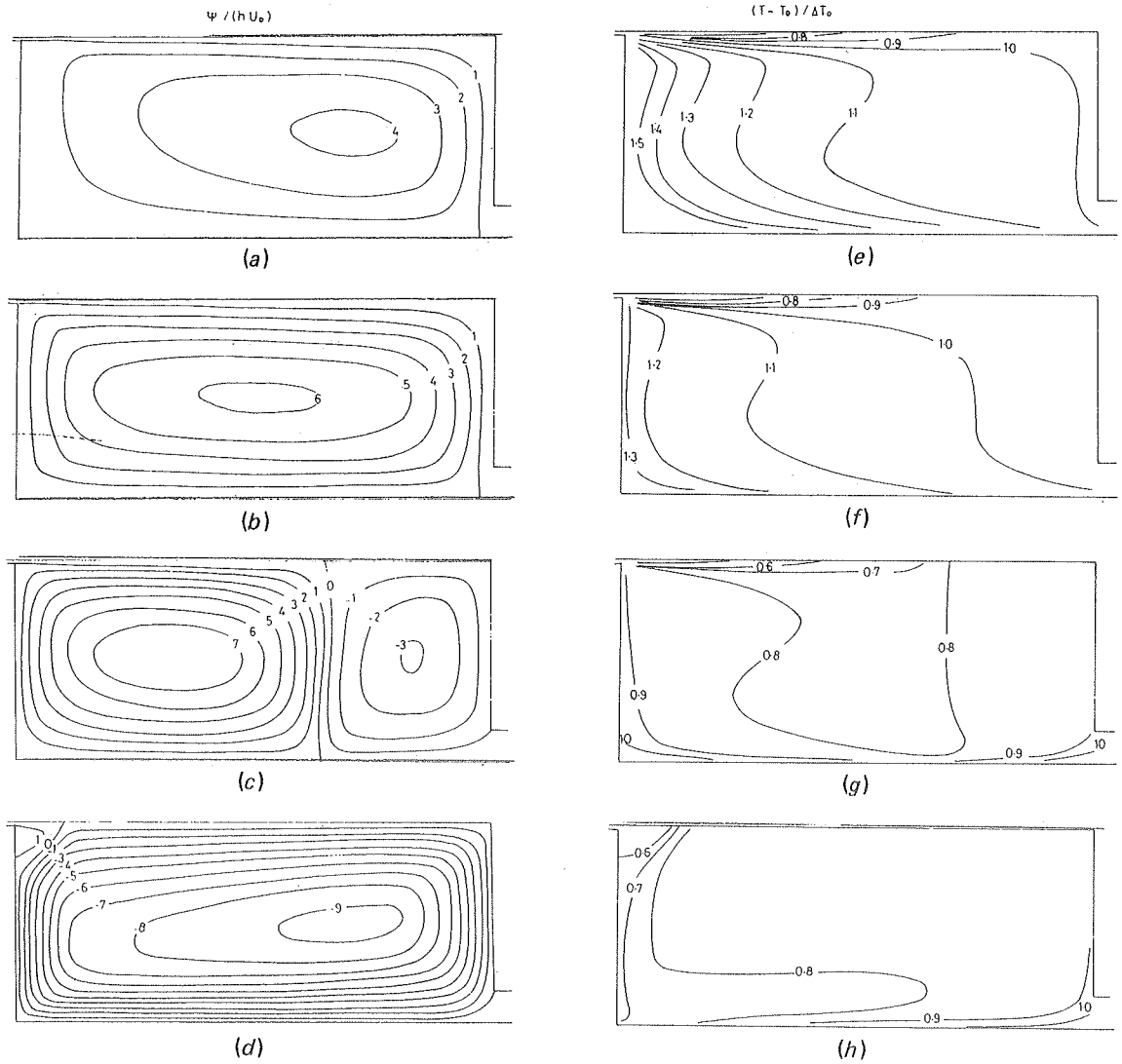

Fig. 2 Patterns of streamlines (*a*–*d*) and isotherms (*e*–*h*) at Re = 7350, $L/H = 3.0$, $h/H = 0.017$, and Ar as follows: (*a* and *e*) 0, (*b* and *f*) 8×10^{-3}, (*c* and *g*) 2×10^{-2}, and (*d* and *h*) 8×10^{-2}.

using meshes of approximately 500 grid nodes. Computing times varied from 100 s in almost isothermal flows to 300 s at high Archimedes numbers. Tests with larger numbers of grid nodes indicated that differences of the order of 2% of the maximum velocity and temperature difference in the flow may be attributed to grid dependence.

CALCULATED RESULTS

The geometric configuration is shown in Fig. 1 and is the same as that employed in [1]. To demonstrate the effect of increasing temperature gradients on the flow, calculations were performed for the case of a uniformly heated floor at four different values of Ar. L/H and h/H were taken as 3.0 and 0.017 and the Reynolds number was fixed at Re = 7350. The results, in the form of streamlines and isotherms, are shown in Fig. 2. It is obvious that an increase in Ar is accompanied by an increase in the strength of the main vortex up to a point where the jet running along the ceiling no

longer remains attached to it. If Ar is further increased, the point of separation is accordingly moved upstream until a main vortex of opposite sign is established.

In the following a uniformly heated floor is assumed. It is the simplest representation of the practical case of a room where the heat dissipated by its occupiers is removed by a continuous flow of fresh air.

From a practical point of view, it is important to establish the relative magnitudes of the contributions of different terms added to the equations to describe buoyancy effects. They are shown in Fig. 3, where the maximum velocity in the return flow U_{rm} is plotted against Ar for the geometry mentioned above and also for L/H, h/H, and Re values of 3.0, 0.056, and 7450. The continuous lines correspond to calculations with the complete equations of Table 1, and the dashed lines to parallel calculations where only the buoyancy term in the V-momentum equation was included. It is obvious that, for both values of h/H, the simpler approach produces results that are a reasonable approximation only at low Ar, where the buoyancy effect is negligible anyway. For this reason, the buoyancy terms have been included in the V, K, and ϵ equations employed in the remaining calculations with buoyancy.

To assess the accuracy of the present method, comparisons with experimental data are necessary. The measurements of Nielsen [2] were obtained at very low Ar ($\sim$1.1 to 3.1×10^{-6}) and with the geometry of Fig. 1 and $L/H = 3.0$ and $h/H = 0.056$. The effects of buoyancy at this value of Ar are very small, as shown by Fig. 3, and the calculated horizontal temperature profiles of Fig. 4, one at the bottom surface of the model and the other at $Y/H = 0.75$, are in very good agreement with the measurements. A constant heat flux distribution was assumed in the flow, in the absence of detailed experimental information, and may be the main cause of the small discrepancies. The foregoing calculations were carried out over the entire flow, instead of prescribing values along a and b of Fig. 1.

However, most of the available experimental data are related to geometries with

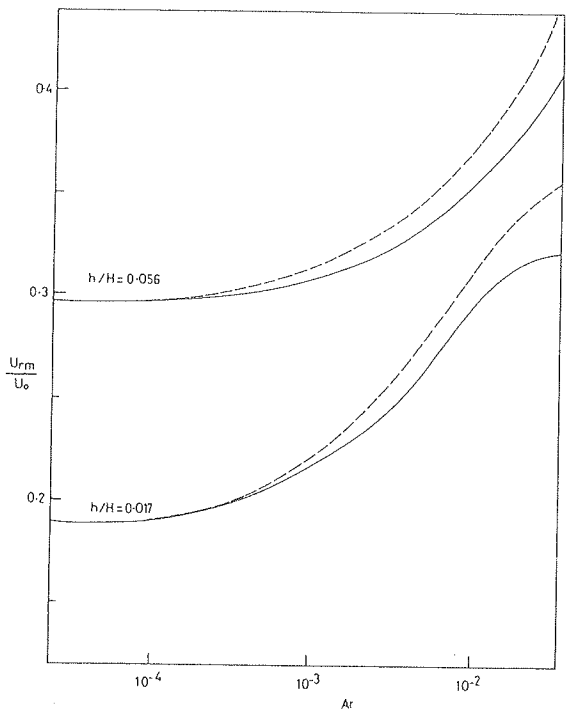

Fig. 3 Comparison of predicted U_{rm}/U_0 versus Ar for $L/H = 3.0$, $h/H = 0.056$ and 0.017, and Re = 7350, with (——) equations as in second section of this paper and (— — —) buoyancy terms ignored, except in momentum equation.

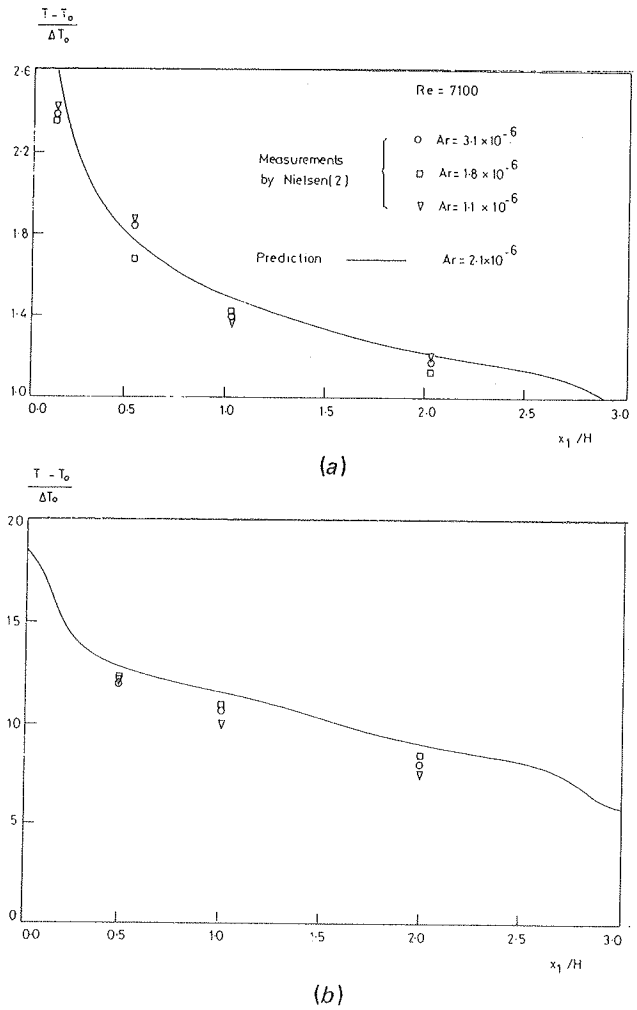

Fig. 4 Temperature profiles at (*a*) $y = 0.75H$ and (*b*) $y = H$ from Nielsen [2].

smaller values of h/H which, when applying the finite-difference scheme, require very refined grids in the vicinity of the inlet plane. The special treatment of this area was described in [1]. The calculations of Fig. 5 show the maximum velocity across the jet U_m at different values of Ar and were obtained without jet development assumptions for $L/H = 3.0$ and $h/H = 0.056$ and 0.017. It is obvious that buoyancy forces distort the velocity field from the first few slot heights downstream of the inlet, and the procedure of [1], used for subsequent calculations, must be regarded as approximate.

The experiments of Hestad [7] are related to a geometry with $h/H = 0.0033$ and were predicted with measured velocity and temperature values along boundary *a* (Fig. 1); other parameters were $L/H = 1.867$, $\mathrm{Re} = 1400$, and $\mathrm{Ar} = 5.5 \times 10^{-4}$. Results are shown in Fig. 6, together with the isothermal prediction from [1], and also in Fig. 7, with the original tracings from Hestad's experiments. As can be seen, U_{rm} is overpredicted by approximately 10%, but the general velocity pattern is reproduced. Temperatures are slightly less well represented, but are satisfactory in view of the strong influence of buoyancy in this flow (equivalent to Fig. 2*c*). Also, the measured isotherms suggest that heat is transferred from the ceiling, and this has not been accounted for in the calculations, where the ceiling was treated as an adiabatic boundary.

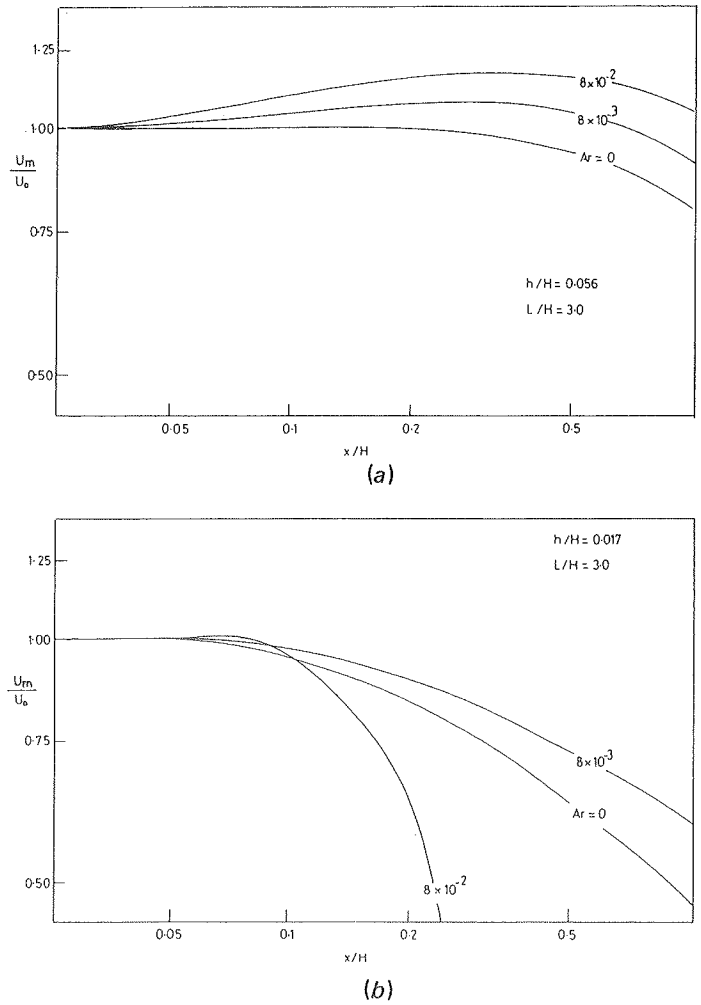

Fig. 5 Decay of maximum velocity in jet for $L/H = 3.0$, Re = 7350, and $h/H =$ (*a*) 0.056 and (*b*) 0.017.

An interesting problem is posed by the experiments of Schwenke [6], who measured the penetration depth x_R of the jet as a function of Ar at several values of h/H and found that, for a limited range of Ar, two different flow patterns were observed with correspondingly different values of x_R. The higher x_R (here designated solution of type I) occurred when Ar was being gradually increased and the lower x_R (type II) when Ar was gradually decreased. In principle, this situation is outside the scope of the present calculation method, since the equations ignore the time dependence of the mean flow. Two solutions may, however, be obtained at certain Ar if approximate distributions of the relevant variables are taken as initial guesses in the iterative procedure. It was found that results of type I occur when the initial guess is a converged solution of a previous calculation obtained for a slightly lower value of Ar; as the Ar of the initial guess is increased the same type of flow exists until the flow pattern finally reverses. Thereafter, results of type II will be obtained for values of Ar higher than the critical value. Solutions of type II are obtained by progressively decreasing the value of the Ar of the initial guess from a higher value. The two types of solutions are indicated in Fig. 8 for $h/H = 3.0$, $h/H = 0.017$, Re = 7450, and Ar = 0.04. Figure 9 presents Schwenke's measurements for $L/H = 1.6$ and $h/H =$ 0.017, together with the present predictions obtained as described above. The

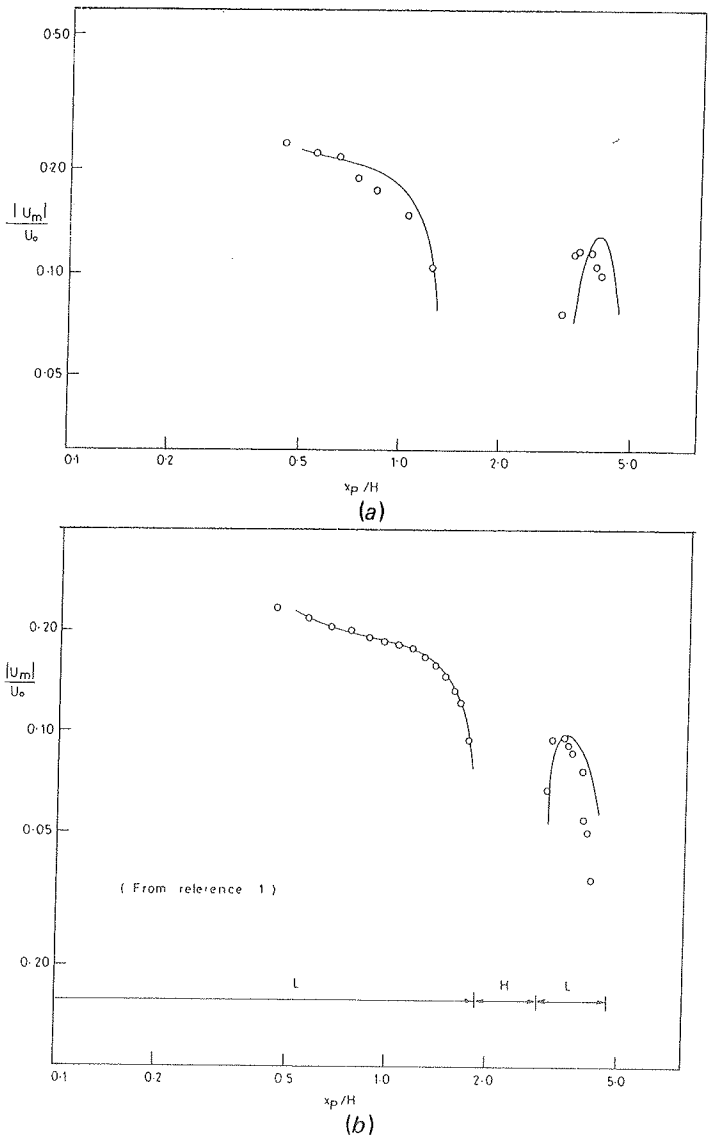

Fig. 6 Maximum velocity along periphery of room: experimental data from Hestad [7] and present prediction. (*a*) Buoyant and (*b*) isothermal.

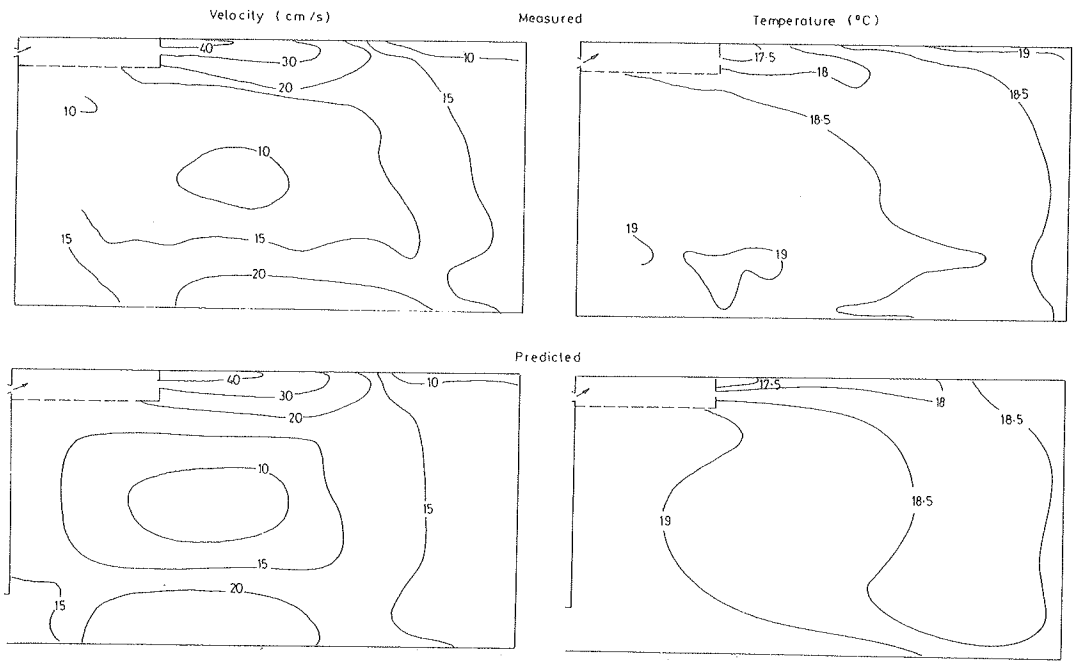

Fig. 7 Patterns of isovels and isothermals: experimental data from Hestad [7] and present prediction.

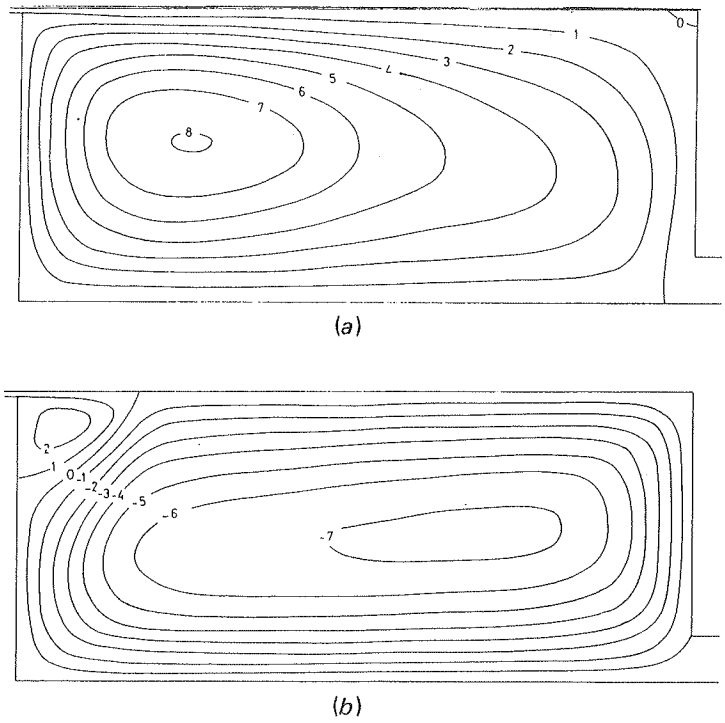

Fig. 8 Predicted flow patterns at $Ar = 4 \times 10^{-2}$: (*a*) type I and (*b*) type II (see text); $L/H = 3.0$, $h/H = 0.017$, and $Re = 7350$.

agreement is less satisfactory than in the previous cases, but the main pattern is once more reproduced.

Comparisons of Figs. 4, 6, 7, and 9 form the basis for an evaluation of the proposed numerical approach and, with the resulting knowledge of the likely precision of the method, calculations were performed outside the range of existing measurements and are intended to provide guidelines for the designer of air-conditioning systems. The

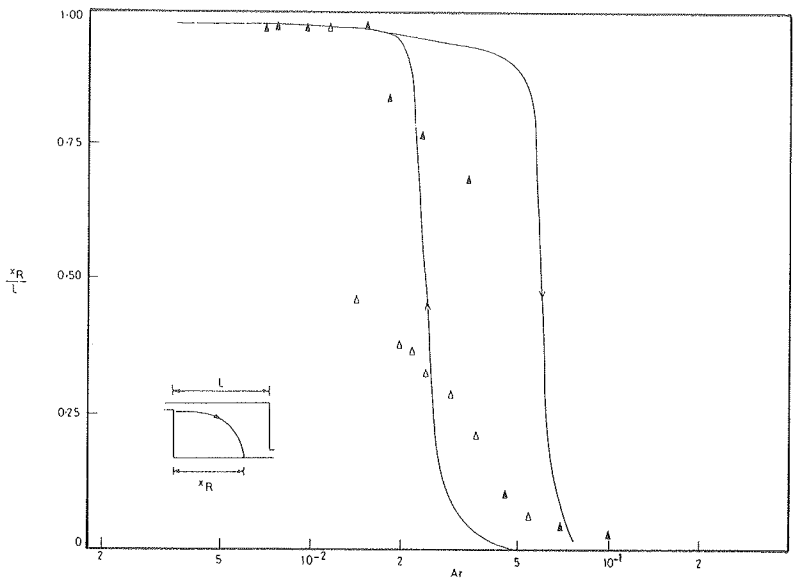

Fig. 9 Dependence of penetration depth x_R on Ar: data from Schwenke [6] and present prediction; $L/H = 1.6$ and $h/H = 0.017$.

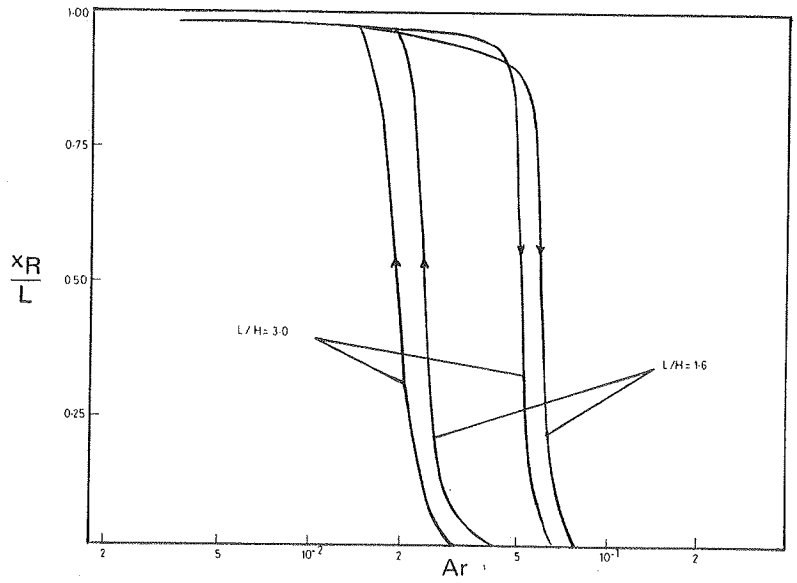

Fig. 10 Dependence of penetration depth x_R on L/H at different Ar (prediction); $h/H = 0.017$.

influence of the length-to-height ratio of rooms, as a function of Ar, is shown in Fig. 10. Increasing L/H from 1.6 to 3.0 is shown to have a relatively small influence in the range of Ar where the inversion of flow pattern occurs. Figure 11 is a generalization of a similar chart presented in [1] for isothermal flows. The maximum velocity in the reverse flow, normalized by the inlet velocity, is plotted against h/H for Ar of 5×10^{-4}, 10^{-3}, and 5×10^{-3}. Values of h/H lower than 0.015 are not included because of the difficulty pointed out earlier, associated with narrow slots. A uniform heat flux over the bottom surface was again assumed.

Figures 10 and 11 indicate that the maximum velocity in the reverse flow increases with the heat load in a ventilated room, and at high heat loads buoyancy leads to an inverse flow pattern. The Ar at which this inversion occurs is almost independent of the room length, and the values of Ar required to produce substantial effects on the flow patterns decrease with the relative slot size h/H.

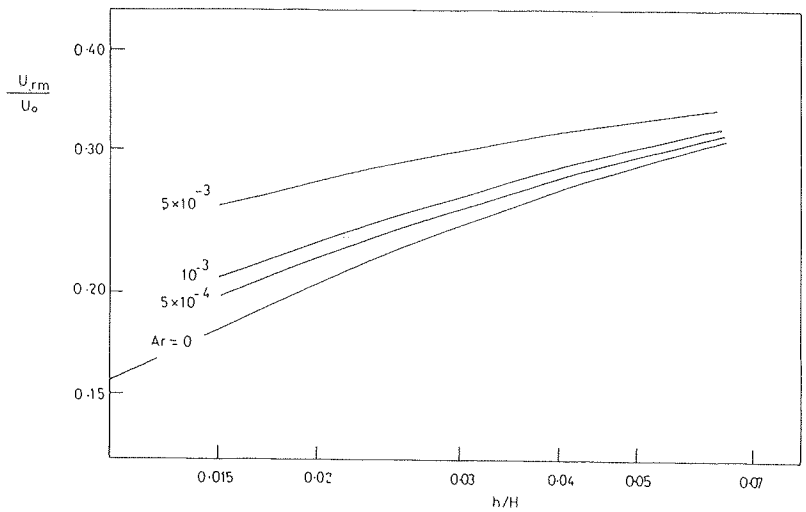

Fig. 11 Dependence of maximum velocity in reverse flow U_{rm} on slot height and Ar (prediction); $L/H = 3.0$.

CONCLUSIONS

Prediction of buoyancy-affected flows in ventilated rooms has been demonstrated in a wide range of room geometries and with different heat loads, using the effective viscosity $K-\epsilon$ model of turbulence. The main conclusions are as follows.

Up to the highest Ar investigated–i.e., 0.08 and 0.00055 in geometries with $h/H = 0.017$ and 0.0033, respectively–which correspond to flow patterns strongly distorted by buoyancy, the degree of accuracy is shown to be adequate for design purposes. In the latter case agreement with experimental data is within 4% of the maximum velocity and 5% of the maximum temperature difference in the flow.

Part of the quoted uncertainty results from grid dependence in the calculations, estimated as 2% for both properties. The remainder may be attributed to the empirical assumptions in the turbulence model and wall functions employed, and also to the simplified treatment of the inlet region. Improvements may be expected from the solution of transport equations for the turbulent stresses and heat fluxes, particularly in strongly buoyant flows where the concepts of eddy diffusivities are less adequate, but the added computational work and cost involved are not justifiable for most practical applications. Developments in the ability to prescribe correct boundary conditions for the inlet region in more general circumstances are likely to produce more significant improvements.

The predicted results quantify the effects of buoyancy and their dependence on the geometric ratios h/H and L/H. They show, for example, that increasing L/H from 1.6 to 3.0 decreases by only 20% the range of Ar where reversal of the flow occurs, and that an Ar of 5×10^{-4} results in a maximum reverse velocity at $h/H = 0.05$, which is identical to that for isothermal flow, but in a value larger by 25% in a geometry with $h/H = 0.015$.

REFERENCES

1. P. V. Nielsen, A. Restivo, and J. H. Whitelaw, The Velocity Characteristics of Ventilated Rooms, *J. Fluids Eng., Trans. ASME*, vol. 100, p. 291, 1978.
2. P. V. Nielsen, Flow in Air Conditioned Rooms (English translation of Ph.D. thesis, Technical Univ. of Denmark, 1974), Danfoss A/S, Denmark, 1976.
3. M. Larson, Predictions of Buoyancy Influenced Flow in Ventilated Industrial Halls, *Proc. Heat Transfer in Buildings, Dubrovnik*, 1977.
4. W. Linke, Strömungsvorgänge in zwangsbelüfteten Räumen, *VDI Ber. (Ver. Dtsch. Ing.)*, vol. 21, p. 29, 1957.
5. P. J. Jackman, Air Movement in Rooms with Ceiling-Mounted Diffusers, Heating and Ventilating Research Association, Lab. Rept. 81, 1973.
6. H. Schwenke, Das Verhalten ebener horizontaler Zuluftstrahlen im begrenzten Raum, dissertation, Technical Univ. of Dresden, 1973.
7. T. Hestad, private communication, Farex Fabrikker A/S, Norway, 1974.
8. Y. Nagasawa, Strömungs- und Temperaturverhältnisse in einem Modellraum mit Bodenheizung, Lehrstuhl für Wärmeübertragung und Klimatechnik RWTH, Aachen, 1974.
9. B. E. Launder, Proposals for Incorporation of Buoyancy Effects into the $K-\epsilon$ Model of Turbulence, private communication, Imperial College, 1973.

10. M. M. Gibson and B. E. Launder, Ground Effects on Pressure Fluctuations in the Atmospheric Boundary Layer, *J. Fluid Mech.*, vol. 86, p. 491, 1978.
11. A. D. Gosman and W. M. Pun, lecture notes for a course entitled Calculation of Recirculating Flows, Imperial College, Heat Transfer Sect., Rept. HTS/74/3, 1974.

Requests for reprints should be sent to J. H. Whitelaw.